# Reversible Activation of Diblock Copolymer Monolayers at the Interface by pH Modulation, 2: Membrane Interactions at the Solid/Liquid Interface

**Florian Rehfeldt,*,†,▽ Roland Steitz,‡ Steven P. Armes,§ Regine von Klitzing,|| Alice P. Gast,⊥ and Motomu Tanaka*,†,#**

*Physik Department E22, Technische Universität München, James-Franck-Str., D-85748 Garching, Germany, Hahn-Meitner-Institut Berlin GmbH, BENSC SF1, Glienicker Str. 100, Berlin D-14109, Germany, Department of Chemistry, Dainton Building, University of Sheffield, Brook Hill, Sheffield, South Yorkshire S3 7HF, UK, Universität Kiel, Institut für Physikalische Chemie, Ludewig-Meyn-Str. 8, D-24118 Kiel, Germany, Department of Chemical Engineering, Massachusetts Institute of Technology, Cambridge, Massachusetts 02139, and Institute of Physical Chemistry, University of Heidelberg, D-69120 Heidelberg, Germany*

*Received: August 12, 2005; In Final Form: March 13, 2006*

A monolayer of the pH-responsive poly[2-(dimethylamino)ethyl methacrylate-*block*-methyl methacrylate] diblock copolymer [PDMAEMA-PMMA] was transferred from the air/water interface to a silicon substrate for evaluation as a tunable interlayer between biological material and solid substrates. Specular neutron reflectivity experiments revealed that the weak polyelectrolyte PDMAEMA chains at the solid/liquid interface can be reversibly activated by pH modulation. The thickness, scattering length density, and surface roughness of the polymer film can be systematically controlled by pH titration. As a simple model of plasma membranes, a lipid bilayer was deposited onto the polymer film. The membrane−substrate interaction was characterized by neutron reflectivity experiments, demonstrating that the membrane−substrate distance could be reversibly regulated by pH titration. These results confirm the potential of stimuli-responsive polymers for precise control of cell−surface interactions.

## Introduction

Biocompatible interlayers that can connect solids and soft biological materials are important in numerous scientific and practical applications.[1−3] For this purpose, lipid bilayer membranes deposited either directly on solids or on ultrathin polymer supports have been widely used as model cell surfaces.[1,4] In the latter case, soft cushions that mimic the generic role of the extracellular matrix (ECM) and glycocalix can provide a water reservoir that prevents direct protein−substrate contacts, and hence reduces the risk of protein denaturation. In nature, neighboring cells and tissue maintain a certain distance (typically in the range of 10−100 nm) to avoid direct, nonspecific contacts as well as to create hydrodynamic pathways. This is achieved by a complex interplay of short- and long-range forces operating within hydrated layers such as the ECM[5] and the cell−surface glycocalix.[6] The long-range forces operating across thin interlayers include van der Waals (dispersion) forces, electrostatic forces, steric (entropic) forces, and hydration forces.[7,8] Major requirements for these interlayers include hydration properties, well-defined film thicknesses, and surface topographies.

For the design of ECM and glycocalix models, the straightforward strategy is the direct use of natural ECM components such as laminin, fibronectin, and hyaluronan;[5,9] however, the physical properties of these natural macromolecular complexes are not easily controlled. Coating surfaces with hygroscopic polymers or hydrogels, such as dextran[10] and poly(ethylene glycol) (PEG) brushes,[11] is another promising approach. Owing to steric forces, such films resist nonspecific adsorption of proteins.[12−15] This effect has been exploited in numerous fields, although such steric layers are known to induce large fluctuations that destabilize the cell−surface contact, so that cells and lipid membranes are repelled from the surface.[16] In a third approach, many studies have utilized multilayers of strong polyelectrolyte films as polymer interlayers.[17,18] Such films can be produced by layer-by-layer deposition by using cationic and anionic polyelectrolytes. The disadvantage of this method arises from the fact that most of these polyelectrolyte complexes are based on strong polyelectrolytes carrying extremely high charge densities over wide pH ranges. These highly charged surfaces lead to undesirably strong electrostatic interactions with cells and proteins. In a previous study, we found that adult mammal cell membranes (derived from human erythrocytes) were strongly pinned to the surface of a commonly used polycation (poly-L-lysine) due to its high charge density; this problem can be interpreted in terms of dewetting of the cell membranes.[19]

We have also been using thin films of regenerated cellulose to accommodate both artificial and native cell membranes.[19−23] These films can be prepared either by spin-coating or by Langmuir−Blodgett deposition of synthetically modified cellulose, followed by chemical regeneration to recover the original cellulose.[23] Both methods enable us to control the film thickness within nanometer accuracy, while maintaining very small

* Corresponding authors. E-mail: frehfeld@ph.tum.de (F.R.); tanaka@uni-heidelberg.de (M.T.). Telephone: +49 (89) 28 91 24 95 (F.R.); +49 (6221) 54 49 16 (M.T.). Fax: +49 (89) 28 91 24 69 (F.R.); +49 (6221) 54 49 50 (M.T.).

† Physik Department E22, Technische Universität München.

‡ Hahn-Meitner-Institut Berlin GmbH.

§ Department of Chemistry, Dainton Building, University of Sheffield.

|| Universität Kiel, Institut für Physikalische Chemie.

⊥ Department of Chemical Engineering, Massachusetts Institute of Technology.

# Institute of Physical Chemistry, University of Heidelberg.

▽ Present contact: Biophysical Engineering Lab, University of Pennsylvania, 112 Towne Building, Philadelphia, Pennsylvania 19104-6315. E-mail: rehfeldt@sas.upenn.edu.

10.1021/jp054533b CCC: $33.50 © 2006 American Chemical Society
Published on Web 04/14/2006

topographic roughness (the typical rms roughness is 5 Å and is independent of the total thickness or preparation methods). Previously, we studied the equilibrium swelling behavior of polysaccharide films by ellipsometry under well-defined osmotic pressure conditions.[23] By analyzing the measured force−distance (i.e., osmotic pressure vs thickness) relationships, we found that regenerated cellulose exhibits an apparently smaller characteristic decay length than other polysaccharides such as dextran or hyaluronan.[24] This can be attributed to the tight hydrogen-bonding network between "rodlike" cellulose molecules and, therefore, suggests smaller repulsion forces. Indeed, we achieved thermodynamically and mechanically stable deposition of artificial lipid membranes on cellulose films, in contrast with the results obtained with dextran films. Furthermore, regenerated cellulose consists of electrically neutral glucose; this net zero charge is advantageous compared to that of strong polyelectrolyte films. In fact, we demonstrated homogeneous spreading of human erythrocyte membranes over macroscopically large surfaces, in clear contrast to the dewetting of the cell membranes observed on poly-L-lysine.[19] These results validated our strategy: it is important to control the interplay of the interfacial forces.

A more sophisticated approach would be the use of a polymer whose properties can be modulated by external stimuli.[25−27] For this purpose, weak polyelectrolytes seem more suitable than strong polyelectrolytes because the degree of ionization (d.i.) can be adjusted by pH titration.

Here, we use a diblock copolymer based on poly[2-(dimethylamino)ethyl methacrylate-*block*-methyl methacrylate] (PDMAEMA-PMMA), which consists of an equal number of monomer repeat units ($n = 36$) for the hydrophobic PMMA and hydrophilic PDMAEMA blocks (designated sample code: DB 50). As reported in our previous account,[53] this diblock copolymer forms a stable monolayer at the air/water interface that allows monolayer deposition on solid substrates at well-defined grafting densities. Furthermore, the hydrophilic PDMAEMA component is a weak polyelectrolyte that significantly changes its degree of ionization (d.i.) near physiological conditions. This reversible switching of the d.i. by pH modulation also alters the polymer's conformation and hydration properties and hence its surface free energy.

In this paper, the physical properties of such diblock copolymer monolayers at the solid/liquid interface are examined by specular neutron reflectivity.[28] Neutron reflectometry is sensitive to the contrast in scattering length density and thus allows us to highlight the "layer of interest" by selective deuteration, which is ideal for determining the film thickness, interfacial roughness, and degree of hydration under aqueous environments. Several studies have been conducted to characterize lipid bilayers and multilayers either on solid[29−32] or on polymer supports[33−35] by using neutron reflectometry. To date, all the previous reports deal with "static" systems with fixed membrane−substrate interaction potentials: in situ observation of membrane−surface interactions activated by stimuli-responsive polymer films has not yet been reported. On the basis of our results obtained at the air/water interface,[53] we transfer monolayers of DB 50 from the air/water interface to solid surfaces. By using neutron reflectometry, we demonstrate the reversible activation of DB 50 films at the solid/liquid interface by pH modulation, which can be further exploited to tune the interaction between plasma membranes and solid substrates.

## Experimental Section

**Materials.** The synthesis of the PDMAEMA-PMMA diblock copolymer with 50 mol % DMAEMA monomer (DB 50, $M_w = 9.3$ kDa; $M_w/M_n < 1.10$) was achieved by group transfer polymerization and is described in detail elsewhere.[36] Deionized water from a Milli-Q device (Millipore, Molsheim, France) and $D_2O$ (purity > 99.9%) from Sigma-Aldrich (Munich, Germany) were used throughout this study.

The pH of the subphase was adjusted by titration of phosphate buffered saline (PBS) consisting of 10 mM $NaH_2PO_4$ and 100 mM NaCl. Fully deuterated poly(methyl methacrylate) (d8-PMMA) with a molar mass of 35 kDa and a polydispersity index of 1.10 was purchased from PSS (Mainz, Germany). 1-Stearoyl-2-oleoyl-*sn*-glycero-3-phosphocholine (SOPC) and 1-stearoyl-2-oleoyl-*sn*-glycero-3-phospho-rac-1-glycerol (SOPG) were purchased from Avanti Polar Lipids, Inc. (Alabaster, AL). All other chemicals were purchased from Sigma-Aldrich (Munich, Germany) and used without further purification. Single-side polished silicon (111) blocks ($80 \times 50 \times 15$ mm$^3$) were bought from Siliciumbearbeitung Andrea Holm (Tann, Germany).

**Diblock Copolymer Film.** Langmuir−Schaefer (LS) deposition of a DB 50 monolayer onto a d8-PMMA precursor film is described in our previous account.[53] Briefly, the silicon blocks were cleaned with a modified RCA method[37] and dried in a vacuum chamber. A 10 mg ml$^{-1}$ d8-PMMA solution was deposited on the block to obtain full coverage and then spun at 3500 rpm for 60 s. After storing at 120 °C for 2 h, the DB 50 monolayer was transferred from the air/water interface at pH 5.5. Subsequently the film was dried, rinsed with water to remove the remaining salt, and dried again.

**Supported Lipid Membranes.** A mixture of 50% SOPC and 50% SOPG in $CHCl_3$ solution was prepared in a glass vial. The solvent was evaporated by using a stream of nitrogen, and the vials were stored in a vacuum chamber for at least 8 h. The dried lipids were dispersed in PBS at a concentration of 1 mg ml$^{-1}$ and further incubated at 42 °C for 2 h. The resulting multilamellar vesicle suspension was extruded 11 times by using the LiposoFast LF-1 extruder (Avestin Inc., Ottawa, Canada) with a filter pore diameter of 50 nm to get small ($d \sim 50$ nm) unilamellar vesicles. The vesicle suspension was gently injected into the flow chamber to form the supported bilayer. After 1 h incubation, the flow chamber was rinsed with PBS to remove vesicles from the bulk buffer solution.

**Neutron Reflectivity.** The neutron reflectivity measurements were performed at the V6 reflectometer at the Hahn-Meitner-Institut (HMI) in Berlin (Germany). The detailed description of the instrument is given elsewhere.[38] With a graphite monochromator, the wavelength of the neutrons is selected as $\lambda = 4.66$ Å. A slit system confines the neutron beam to a cross-section of $0.5 \times 40$ mm$^2$ for $q \leq 0.0518$ Å$^{-1}$ and to $1 \times 40$ mm$^2$ for $q > 0.0518$ Å$^{-1}$, yielding an instrument resolution of $\Delta q/q = 0.001$ Å$^{-1}$ and 0.002 Å$^{-1}$, respectively. The scattered neutrons are detected with a $^3$He detector with $\theta/2\theta$ scans from $q = 0.0047-0.1599$ Å$^{-1}$. After each run (requires about 10 h), the first part of the run was repeated ($q = 0.0047-0.0518$ Å$^{-1}$) to confirm the stability of the sample. The acquired data were analyzed by using Parratt's dynamical approach for reflectivity on layered samples.[39] Best-fit values for thickness, interfacial roughness, and scattering length density (SLD) for box models were obtained with the open software Parratt32 (available from the Hahn-Meitner Institute Berlin via http://www.hmi.de/bensc/instrumentation/instrumente/v6/refl/parratt_en.htm).

For the measurements at the solid/liquid interface, a PTFE flow chamber with an inner dimension of ($72 \times 42 \times 3$ mm$^3$) was used.[40] The buffer can be exchanged by gentle rinsing of the chamber with two syringes located at the inlet and outlet. The total volume of the chamber (including tubing inlet and

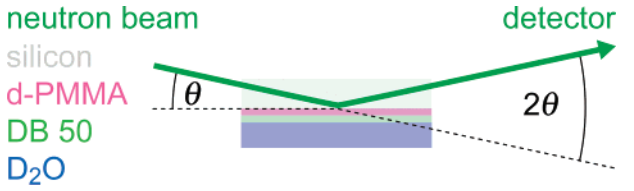


**Figure 1.** Sketch of the experimental setup. The neutron beam enters the silicon block from the side and is reflected at the solid/liquid interface. To enhance the contrast of the "protonated" DB 50 layer, a fully deuterated d-PMMA precursor film was deposited, and $D_2O$ was used as the subphase. The sample is mounted onto a flow chamber for exchange of the subphase.

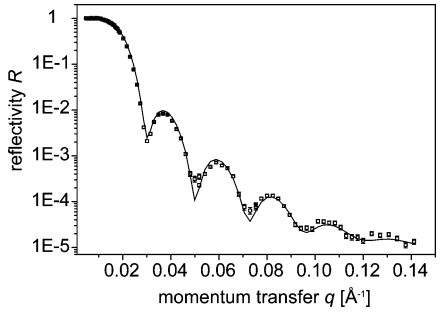


**Figure 2.** Reflectivity curve of a dry DB 50 layer transferred at $\pi =$ 25 mN m$^{-1}$ measured in air. Open squares represent the measured data points, while the solid line is the best fit.

outlet) was approximately 11 mL. To ensure the full exchange of the fluid within the flow chamber, it was rinsed with 5 times the volume. The reflectivity setup is shown schematically in Figure 1.

**Ellipsometry.** The thickness of the polymer layers was measured after each preparation step by using a conventional PCSA (polarizer, compensator, sample, analyzer) ellipsometer (SD 2000, Plasmos GmbH, Germany) at an angle of incidence of 70° and a wavelength of 632.8 nm (He−Ne laser). A refractive index of $n_{Si} = 3.868 - i0.024$[41] was taken for silicon, and $n = 1.49$ for d-PMMA and DB 50.[42]

## Results and Discussion

**Reversible Activation of the Polymer Chains.** Dry precursor layers and diblock copolymer monolayers deposited on the silicon substrates were first characterized with ellipsometry and neutron reflectivity in air. The deviation in the film thicknesses obtained by two techniques was within ± 5 Å (comparable to the roughness of the film, $\sigma \sim 5$ Å), verifying the quality of the sample and the validity of the material parameters taken for the fit. Figure 2 represents the reflectivity curve of DB 50 transferred at a lateral pressure of $\pi = 25$ mN m$^{-1}$ (corresponding to an area per molecule of 435 Å$^2$) onto a silicon block coated with d-PMMA. The use of a relatively thick ($d = 266$ Å) d-PMMA precursor film leads to a shift of periodicity of the Kiessig fringes to smaller $q$-values, which provides a higher signal-to-background ratio. Open squares denote the measured data points, while the solid line represents the best fit with a four-box model consisting of air, DB 50, d-PMMA, and silicon. The thickness (29 Å) and SLD ($1.4 \times 10^{-6}$ Å$^{-2}$) of the dry films are used as reference data for the following experiments in aqueous solution.

After characterization in air, the silicon block was mounted in the flow chamber. Figure 3A represents the neutron reflectivity curves obtained for a DB 50 monolayer at pH 5.5 (red open triangles) and pH 8.5 (black open circles), together with the best fits corresponding to each data set (solid lines). Here,

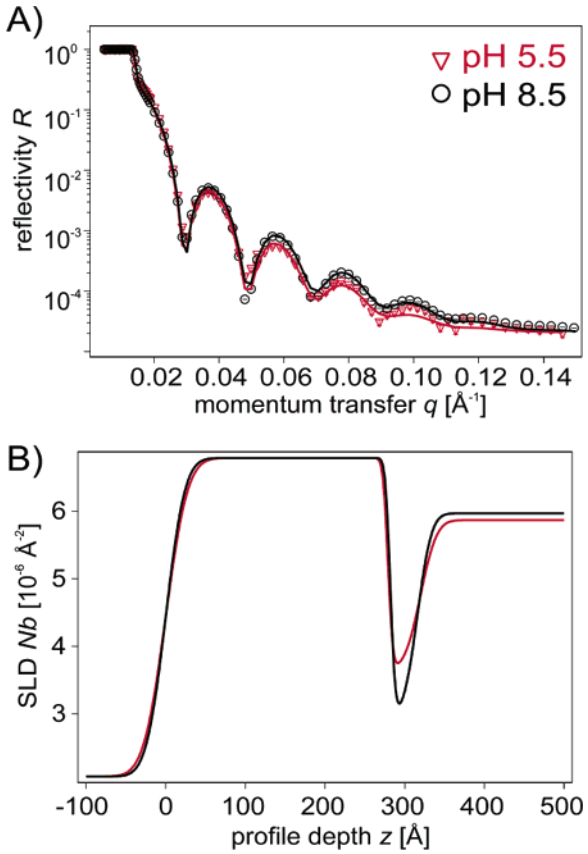


**Figure 3.** (A) Neutron reflectivity curves of DB 50 at pH 5.5 (red open triangles) and pH 8.5 (black open circles). The lines represent the best fit corresponding to the parameters mentioned in Table 2. (B) Plot of the scattering length density *Nb* shown with respect to the depth profile *z*.

**TABLE 1: Molecular Volume *V* and Scattering Length Density *Nb* of Each Layer[43]**

| | $V$ [Å$^3$] | $Nb$ [$10^{-6}$·Å$^{-2}$] |
|---|---|---|
| Si | | 2.07 |
| d-PMMA | 140 | 7.02 |
| MMA | 140 | 1.07 |
| DMAEMA | 225 | 0.80 |
| $D_2O$ | 30 | 6.37 |
| DB 50 | 365 | 0.94 |
| alkyl chains | | −0.37 |

**TABLE 2: Best Fit Parameters for the Results in Figure 3, Based on the 4-Box Model Including Si, d8-PMMA, DB 50, and $D_2O$[a]**

| DB 50 ($\pi = 25$ mN m$^{-1}$) | pH 8.5 | pH 5.5 |
|---|---|---|
| $d_{DB50}$ [Å] | 34 | 41 |
| $\sigma_{DB50}$ [Å] | 14 | 16 |
| $Nb_{DB50}$ [$10^{-6}$ Å$^{-2}$] | 2.95 | 3.65 |
| $\phi_{D_2O}$ | 0.40 | 0.55 |
| $d_{PMMA}$ [Å] | 282 | 279 |
| $\sigma_{PMMA}$ [Å] | 19 | 22 |
| $Nb_{D_2O}$ [$10^{-6}$ Å$^{-2}$] | 5.97 | 5.87 |

[a] SLD values of Si and d8-PMMA in Table 1 were taken and kept constant throughout the fitting.

we measured the same DB 50 film as depicted in Figure 2. The fitted values for layer thickness, SLD, and roughness are summarized in Table 2. The difference in SLD of the subphase to the ideal value of $D_2O$ is due to buffer preparation and titration. The SLD profile measured in the $z$-direction is shown in Figure 3B. Because of the small total layer thickness (30−40 Å), the PMMA and PDMAEMA blocks of the DB 50 film

are treated as one layer (not as two individual layers) in our model. However, the clear contrast in the SLD of the deuterated layers (d-PMMA and $D_2O$) and the protonated DB 50 layer makes the measurement very sensitive to changes in the DB 50 layer.

As reported by An et al.,[44] few (12%) of the DMA side chains are charged at pH 8.5, which leads to the adsorption of "collapsed" PDMAEMA chains to the interface. Here, the thickness, SLD, and the roughness of the uncharged DB 50 layer are: $d = 34$ Å, $Nb = 2.95 \times 10^{-6}$ Å$^{-2}$, and $\sigma = 14$ Å. On the other hand, when the pH is adjusted to pH 5.5 (corresponding to a degree of ionization of 85%), the thickness of the charged DB 50 layer increases to $d = 41$ Å, accompanied with an increase in SLD to $Nb = 3.65 \times 10^{-6}$ Å$^{-2}$. The increase in the DB 50 layer thickness also increases the surface roughness $\sigma$ to 16 Å. This indicates that protonation of the tertiary amine side groups causes desorption of the PDMAEMA chains into the aqueous phase, which is also suggested by the drop in the surface pressure from $\pi = 20$ to 13 mN m$^{-1}$ observed in the in situ pH titration experiments at the air/water interface.[53] Thus the observed increases in thickness, SLD, and roughness of the DB 50 layer seem plausible. The stretching of the charged PDMAEMA chains into water can also be understood in terms of water uptake within the polymer layer. Here, the volume fraction of $D_2O$ ($\phi$) in the polymer layer can be calculated from the experimentally determined scattering length density of the swollen layer $Nb_{swollen}$. This value can be represented as a function of volume fraction of $D_2O$ ($\phi$) and SLD values of $D_2O$ subphase ($Nb_{subphase}$) and dry DB 50 ($Nb_{DB50}$):

$$Nb_{swollen} = \phi \cdot Nb_{subphase} + (1 - \phi) Nb_{DB50} \quad (1)$$

Solving this equation for $\phi$ yields:

$$\phi = \frac{Nb_{swollen} - Nb_{DB50}}{Nb_{subphase} - Nb_{DB50}} \quad (2)$$

By using this equation, the volume fraction $\phi$ of $D_2O$ in the polymer layer is calculated to be 0.40 at pH 8.5 and 0.55 at pH 5.5, respectively. The increase in volume fraction of $D_2O$ from the uncharged to the charged state ($\Delta\phi/\phi = 38\%$) is in reasonable agreement with the observed increase in the DB 50 layer thickness ($\Delta d/d = 20\%$).

In contrast to the films prepared by physisorption from solution,[43] the results presented here (Table 1) demonstrated the clear advantage of monolayers transferred directly from the air/water interface, i.e., the ability to precisely control the lateral density of the polymer chains. The pressure−area isotherms clearly indicate that polymer chain conformations are dependent on the lateral density of the polymer chain, i.e., the surface pressure at which the film is transferred. Unlike the clear changes shown in Figure 3 for the DB 50 film transferred at $\pi = 25$ mN m$^{-1}$ (corresponding to 435 Å$^2$ per molecule), the DB 50 monolayer transferred at $\pi = 35$ mN m$^{-1}$ (338 Å$^2$ per molecule) exhibits almost no difference ($\Delta d$ is less than the surface roughness) upon varying the solution pH between 5.5 and 8.5. This can be explained in terms of the reduced conformational degrees of freedom for the more densely packed PDMAEMA chains. As we observed in our film balance experiments, the difference in area per molecule between pH 5.5 and 8.5 at $\pi = 35$ mN m$^{-1}$ is only 30 Å$^2$ per molecule ($\Delta A/A = 10\%$). In fact, when the film is transferred at a lower surface pressure ($\pi = 15$ mN m$^{-1}$, corresponding to 576 Å$^2$ per molecule), the change in the film thickness was more pronounced ($\Delta d/d \sim 20\%$).

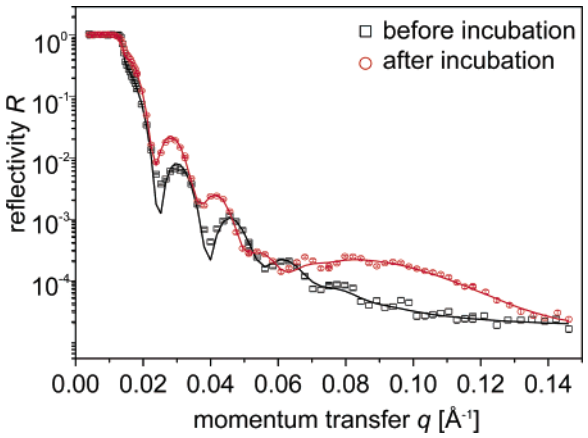


**Figure 4.** Neutron reflectivity curves of a "charged" DB 50 film at pH 5.5 before (black open squares) and after (red open circles) the deposition of a lipid membrane.

For all samples, we repeated the initial part of each scan (from $q = 0.0047$ to 0.0518 Å$^{-1}$) to verify the stability of the film. In all cases, we found that the second scan perfectly overlaps with the first scan. Moreover, we measured the reflectivity of some samples after several pH titration cycles to examine if one can reversibly activate the polymer chain conformation, and we found that the reflectivity curve was reproducible even after five titration cycles (i.e., after 3 days). Thus, we conclude that all the transferred DB 50 films have sufficiently high stabilities to undergo reversible activation of the polymer chain conformation during several pH titration cycles.

**Control of Membrane−Substrate Interaction.** To examine the possibility of fine-tuning cell−substrate interactions, we examined whether the pH-induced activation of PDMAEMA chains can alter their interaction with lipid bilayer membranes, which are the most fundamental component of plasma membranes. To mimic the extracellular leaflet of adult animal cells (which possess anionic character owing to their sialic acid residues), we chose a lipid mixture composed of 50% neutral lipids (SOPC) and 50% negatively charged lipids (SOPG). As both lipids have a phase transition temperature, $T_m$, of approximately 6 °C,[45] the membrane is in the fluid phase under our experimental conditions ($T = 20$ °C). Spreading of lipid vesicles and formation of a homogeneous membrane on the polymer support was confirmed by fluorescence microscopy prior to the neutron reflectivity experiments. Independent of the pH (pH 5.5 and 8.5) and transfer pressures ($\pi = 15$, 25, 35 mN m$^{-1}$), we confirmed that a homogeneous and fluid lipid bilayer was formed on the polymer support (see Supporting Information for fluorescence image of SOPC layer on DB 50 transferred at 25 mN m$^{-1}$ at pH 5.5).

In Figure 4, the reflectivity curves of a "charged" DB 50 film before (black open squares) and after (red open circles) the deposition of a lipid membrane measured at pH 5.5, reveal a significant change in the global shape of the reflectivity curve due to the presence of a lipid membrane. As presented in Figure 5, the titration of pH from pH 5.5 (red open triangles) to 8.5 (blue open circles) leads to a further change in the reflectivity. It should be noted that the reverse pH titration to 5.5 results in recovery of the same reflectivity curve, confirming that the pH-induced conformational change is also reversible in the presence of a lipid membrane.

To interpret the reflectivity curve in the presence of a lipid membrane, we introduced two more boxes to our model: a lipid membrane and a (deuterated) water reservoir between membrane and polymer layer. Here, hydrocarbon chains and phospholipid

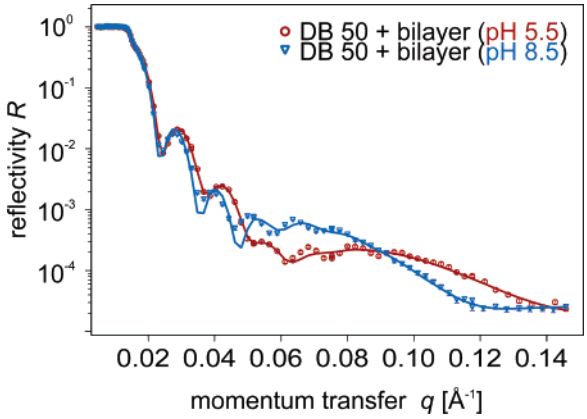


**Figure 5.** Reflectivity curves of the DB 50 film in the presence of a lipid membrane measured at pH 5.5 (red open triangles) and pH 8.5 (blue open circles). Solid lines coincide with the best fit results based on the optimized parameters presented in Table 3.

**TABLE 3: Best Fit Parameters for the DB 50 Film in the Presence of a Lipid Membrane at pH 5.5 and 8.5, Corresponding to the Experimental Results Presented in Figures 4 and 5**[a]

| DB 50 + lipid bilayer | pH 8.5 | pH 5.5 |
|---|---|---|
| $d_{DB50}$ [Å] | 31 | 37 |
| $\sigma_{DB50}$ [Å] | 14 | 17 |
| $d_{D_2O}$ [Å] | 38 | 21 |
| $\sigma_{D_2O}$ [Å] | 14 | 8 |
| $d_{bilayer}$ [Å] | 34 | 28 |
| $Nb_{bilayer}$ [$10^{-6}$ Å$^{-2}$] | 0.41 | 0.30 |
| $\sigma_{bilayer}$ [Å] | 14 | 11 |

[a] SLD of bulk subphase and water gap was kept constant.

headgroups were considered as one layer to reduce the number of boxes in the model. On the other hand, we found that the presence of a $D_2O$ reservoir (including lipid headgroups immersed into water) between the polymer layer and the membrane is a prerequisite for the data interpretation. In fact, other models that do not take the water reservoir into account fail to account for the experimental data. The best fits are presented as solid lines in Figures 4 and 5, and the corresponding fitting parameters are given in Table 3. The scattering length density profiles in the *z*-direction are shown in Figure 6. Here, we kept the SLD of the subphase constant as $Nb = 6.2 \times 10^{-6}$ Å$^{-2}$. During the first fitting, the SLD of the lipid bilayer box was fixed to be $Nb = -1 \times 10^{-6}$ Å$^{-2}$. To achieve the final fitting results, either SLD or thickness was varied, and the fitting cycle was successively repeated until they reached consistent values. Despite several attempts, the quality of the fitting results could not be improved. This might be attributed to the resolution limit of the instrument: the statistical error in reflectivity increases due to the decreasing signal to background noise ratio at $q > 0.065$ Å$^{-1}$.

The fitting results indicate the decrease in the polymer film thickness caused by the deposition of a lipid membrane ($\Delta d = 3-4$ Å), which can be explained in terms of van der Waals forces in multiple interfaces.[7,8] If one roughly assumes a Hamaker constant of a lipid membrane of $10^{-20}$ J (taken from the value for hydrocarbon chains in water),[8] the decrease in the polymer layer thickness can be attributed to the presence of an additional lipid membrane. It should be noted that the Hamaker constant of the swollen DMAEMA block, especially in the presence of additional salts, can hardly be measured. On the other hand, the change in the whole DB 50 layer thickness ($\Delta d = 6$ Å) is similar to that observed in the absence of a lipid membrane, implying that the activation of polymer chain

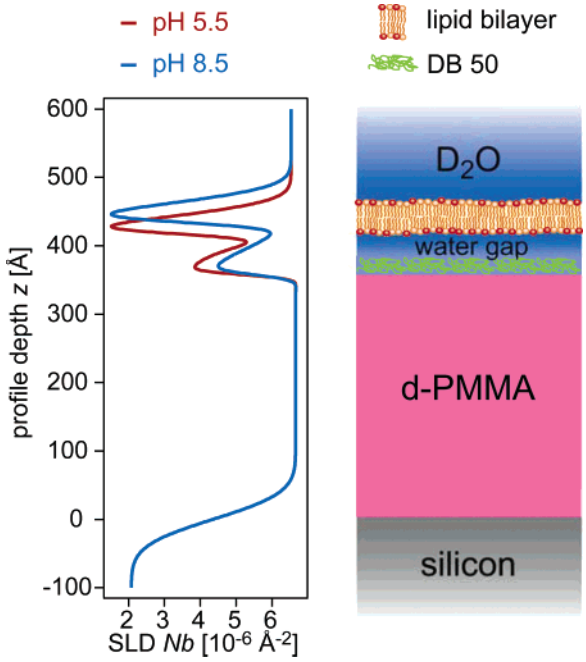


**Figure 6.** The scattering length density *Nb* profile obtained in the *z*-direction, corresponding to the results at pH 5.5 (red) and pH 8.5 (blue).

conformation is relatively unchanged in the presence of a lipid membrane. The fitting results also imply that the membrane thickness on the charged DB 50 film at pH 5.5 is smaller than that on uncharged film at pH 8.5, which can be attributed qualitatively to the compression of the fluid hydrocarbon chains by the increasing polymer−membrane attraction. However, as explained above, such a change obtained from the self-consistent fitting should not be exaggerated. By contrast, the thickness and roughness of the water reservoir are almost independent from the fitting parameters.

Interestingly, if one compares the parameters of each layer at pH 5.5 and 8.5, the most pronounced change appears in the thickness of the $D_2O$ reservoir. At pH 5.5, the reservoir thickness between the membrane and the "charged" polymer layer is $d_{D_2O} = 21$ Å. pH adjustment to 8.5 results in a clear expansion of the $D_2O$ reservoir between the membrane and the "uncharged" polymer layer ($d_{D_2O} = 38$ Å). To date, the thickness of water reservoir for the supported membrane directly deposited onto solid substrates (called solid supported membranes) was measured by several experimental techniques including NMR,[46] fluorescence interference technique,[47] and neutron reflectivity.[48,49] The thickness of water reservoir between the solid surface and the membranes, ranging from 5 to 20 Å, coincides with the position of a deep potential minimum governed by the van der Waals force. When the membrane is further separated by the presence of interlayers, such as hydrated polymers, the membrane can find another potential minimum.[4,50] However, it has been still unclear if a water reservoir exists between the membrane and the polymer support. From this context, our results demonstrate that neutron reflectivity can identify the hydrated polymer film and $D_2O$ reservoir by the contrast in scattering length densities. The sum of the thickness of DB 50 layer and that of the water reservoir ($d_{DB50} + d_{D_2O} = 59-69$ Å) in this study is larger than the typical value found for solid supported membranes ($d_{D_2O} = 5-20$ Å), which clearly proves the active role of polymer supports in adjusting the membrane−substrate interaction.

As reported previously,[44] 85% of the DMAEMA groups are positively charged at pH 5.5, and the degree of protonation

decreases to 12% at pH 8.5. On the other hand, the net charge on the mixed SOPC/SOPS membrane is negative under both pH conditions because the p$K_a$ value of phosphatidylserine in a phosphatidylcholine matrix is about $3.6 \pm 0.1$.[51] Thus these results indicate that the collapse of "uncharged" polymer chains by pH titration from 5.5 to 8.5 decreases the electrostatic attraction between the oppositely charged membranes and polymer films, resulting in a significant increase in the water reservoir thickness (Figure 6). We also checked the stability of the membrane in each state by repeating the first part of each scan, verifying that the change observed here did not coincide with desorption of the lipid membrane. Thus, we conclude that the tuning of interaction potentials between the membrane and the substrate using a diblock copolymer (DB 50) with a weak polyelectrolyte block is advantageous over supported membranes on strong polyelectrolyte films[33−35] or on solid substrates,[29−32] owing to their capability in modulating the membrane−substrate interactions. Further studies with off-specular neutron scattering will enable us to obtain more detailed insights regarding the influence of the adjustment of interfacial potentials on dynamic fluctuation and mechanical properties of supported lipid membranes.[52]

## Conclusions

Specular neutron reflectivity experiments demonstrate that diblock copolymer (DB 50) monolayers transferred to hydrophobic substrates can be reversibly activated by pH modulation. Deposition of insoluble (i.e., Langmuir-type) monolayers of DB 50 at well-defined surface pressures makes it possible to control the lateral chain density precisely, which was found to be a prerequisite to achieve a clear contrast in the polymer chain conformation at "charged" and "uncharged" states. We deposited a lipid bilayer membrane on the DB 50 film and found that the pH activation of these polymer films can regulate the electrostatic interaction at the interface, i.e., the thickness of water reservoir between the membrane and the polymer film. Our results clearly demonstrate the potential of such "tailored" polymer films for the regulation of cell−substrate interaction potentials via external stimuli.

**Acknowledgment.** F.R. and M.T. thank E. Sackmann for fruitful discussions and HMI Berlin for neutron beam time. M.T. thanks the DFG (Emmy Noether Program and French-German Network) and NSF-MRSEC (CPIMA) for the financial support. F.R. thanks H. Schirmer, E. Schneck, and K. Seidel for experimental assistance. A.P.G. acknowledges the support of the Alexander von Humboldt Stiftung for her stays in Germany.

**Supporting Information Available:** Fluorescence microscopy image of a DB 50 monolayer transferred at $\pi = 25$ mN m$^{-1}$ incubated with a SOPC vesicle suspension at pH 5.5. This material is available free of charge via the Internet at http://pubs.acs.org.

## References and Notes

(1) Sackmann, E. *Science* **1996**, *271*, 43.
(2) Sackmann, E.; Tanaka, M. *Trends Biotechnol.* **2000**, *18*, 58.
(3) Tanaka, M.; Rehfeldt, F.; Schneider, M. F.; Mathe, G.; Albersdörfer, A.; Neumaier, K. R.; Purrucker, O.; Sackmann, E. *J. Phys. Condens. Matter* **2005**, *17*, S649.
(4) Tanaka, M.; Sackmann, E. *Nature* **2005**, *437*, 656.
(5) Comper, W. D. *Extracellular Matrix*; Harwood Academic Publishers: Amsterdam, 1996.
(6) Gabius, H. J.; Gabius, S. *Glycoscience*; Chapmann & Hall: Weinheim, 1997.
(7) Derjaguin, B. V.; Churaev, N. V. *Surface Forces*; Consultants Bureau: New York, 1987.
(8) Israelachvili, J. N. *Intermolecular and Surface Forces with Applications to Colloidal and Biological Systems*; Academic Press Inc.: London, 1985.
(9) Fromherz, P. *ChemPhysChem* **2002**, *3*, 276.
(10) Löfas, S.; Johnson, B. *J. Chem. Soc., Chem. Commun.* **1990**, *21*, 1526.
(11) Harris, J. M. *Poly(ethyleneglycol) Chemistry*; Plenum Press: New York, 1992.
(12) Andrade, J. D.; Hlady, V. *Adv. Polym. Sci.* **1986**, *79*, 1.
(13) Herren, B. J.; Shafer, S. G.; Alstine van, J.; Harris, J. M.; Snyder, R. T. *J. Colloid Interface Sci.* **1987**, *115*, 46.
(14) Yang, Z.; Galloway, J. A.; Yu, H. *Langmuir* **1999**, *15*, 8405.
(15) Halperin, A. *Langmuir* **1999**, *15*, 2525.
(16) Elender, G.; Kühner, M.; Sackmann, E. *Biosens. Bioelectron.* **1996**, *11*, 565.
(17) Decher, G. *Science* **1997**, *277*, 1232.
(18) Möhwald, H. *Colloids Surf. A* **2000**, *171*, 25.
(19) Tanaka, M.; Kaufmann, S.; Nissen, J.; Hochrein, M. *Phys. Chem. Chem. Phys.* **2001**, *3*, 4091.
(20) Hillebrandt, H.; Wiegand, G.; Tanaka, M.; Sackmann, E. *Langmuir* **1999**, *15*, 8451.
(21) Goennenwein, S.; Tanaka, M.; Hu, B.; Moroder, L.; Sackmann, E. *Biophys. J.* **2003**, *85*, 846.
(22) Tanaka, M.; Wong, A. P.; Rehfeldt, F.; Tutus, M.; Kaufmann, S. *J. Am. Chem. Soc.* **2004**, *126*, 3257.
(23) Rehfeldt, F.; Tanaka, M. *Langmuir* **2003**, *19*, 1467.
(24) Mathe, G.; Albersdörfer, A.; Neumaier, R.; Sackmann, E. *Langmuir* **1999**, *15*, 8726.
(25) Zhu, X.; De Graaf, J.; Winnik, F. M.; Leckband, D. *Langmuir* **2004**, *20*, 1459.
(26) Auguste, D. T.; Armes, S. P.; Brzezinska, K. R.; Deming, T. J.; Kohn, J.; Prud'homme, R. K. *Biomaterials*, **2006**, *27*, 2599.
(27) Galaev, I. Y.; Mattiasson, B. *Trends Biotechnol.* **1999**, *17*, 335.
(28) Thomas, R. K. *Annu. Rev. Phys. Chem.* **2004**, *55*, 391.
(29) Kuhl, T. L.; Majewski, J.; Wong, J.; Steinberg, S.; Leckband, D. E.; Israelachvili, J. N.; Smith, G. S. *Biophys. J.* **1998**, *75*, 2352.
(30) Charitat, T.; Bellet-Amalric, E.; Fragneto, G.; Graner, F. *Eur. Phys. J. B* **1999**, *8*, 583.
(31) Fragneto-Cusani, G. *J. Phys. Condens. Matter* **2001**, *13*, 4973.
(32) Gutberlet, T.; Steitz, R.; Fragneto, G.; Klosgen, B. *J. Phys. Condens. Matter* **2004**, *16*, S2469.
(33) Ma, C.; Srinivasan, M. P.; Waring, A. J.; Lehrer, R. I.; Longo, M. L.; Stroeve, P. *Colloids Surf. B* **2003**, *28*, 319.
(34) Wong, J. Y.; Majewski, J.; Seitz, M.; Park, C. K.; Israelachvili, J. N.; Smith, G. S. *Biophys. J.* **1999**, *77*, 1445.
(35) Majewski, J.; Wong, J. Y.; Park, C. K.; Seitz, M.; Israelachvili, J. N.; Smith, G. S. *Biophys. J.* **1998**, *75*, 2363.
(36) Baines, F. L.; Billingham, N. C.; Armes, S. P. *Macromolecules* **1996**, *29*, 3416.
(37) Kern, W.; Puotinen, D. A. *RCA Rev.* **1970**, *31*, 187.
(38) Mezei, F.; Golub, R.; Klose, F.; Toews, H. *Physica B* **1995**, *213*, 898.
(39) Parratt, L. G. *Phys. Rev.* **1954**, *95*, 359.
(40) Howse, J. R.; Manzanares-Papayanopoulos, E.; McLure, I. A.; Bowers, J.; Steitz, R.; Findenegg, G. H. *J. Chem. Phys.* **2002**, *116*, 7177.
(41) Tompkins, H. G. *A User's Guide to Ellipsometry*; Academic Press: San Diego, 1993.
(42) Seferis, J. C. Refractive Indices of Polymers. In *Polymer Handbook*; Brandrup, J., Immergut, E. H., Grulke, E. S., Eds.; Wiley: New York, 1999.
(43) An, S. W.; Su, T. J.; Thomas, R. K.; Baines, F. L.; Billingham, N. C.; Armes, S. P.; Penfold, J. *J. Phys. Chem. B* **1998**, *102*, 387.
(44) An, S. W.; Thomas, R. K. *Langmuir* **1997**, *13*, 6881.
(45) Silvius, J. R. Thermotropic Phase Transitions of Pure Lipids in Model Membranes and their Modification by Membrane Proteins. In *Lipid−Protein Interactions*; Wiley−Interscience: New York, 1982; Vol. 2, p 239
(46) Bayerl, T. M.; Bloom, M. *Biophys. J.* **1990**, *58*, 357.
(47) Lambacher, A.; Fromherz, P. *Appl. Phys. A* **1996**, *63*, 207.
(48) Johnson, S. J.; Bayerl, T. M.; McDermott, D. C.; Adam, G. W.; Rennie, A. R.; Thomas, R. K.; Sackmann, E. *Biophys. J.* **1991**, *59*, 289.
(49) Koenig, B. W.; Krueger, S.; Orts, W. J.; Majkrzak, C. F.; Berk, N. F.; Silverton, J. V.; Gawrisch, K. *Langmuir* **1996**, *12*, 1343.
(50) Bruinsma, R.; Sackmann, E. *C. R. Acad. Sci., Ser. IV: Phys. Astrophys.* **2001**, *2*, 803.
(51) Tsui, F.; Ojcius, D.; Hubbell, W. *Biophys. J.* **1986**, *49*, 459.
(52) Salditt, T.; Munster, C.; Mennicke, U.; Ollinger, C.; Fragneto, G. *Langmuir* **2003**, *19*, 7703.
(53) Rehfeldt, F.;Steitz, R.; Armes, S. P.; von Klitzing, R.; Gast, A. P.; Tanaka, M. *J. Phys. Chem. B* **2006**, *110*, 9171.